DFTT 47/96
Cavendish–HEP–96/11
July 1996

Higgs signals and hard photons at the Next Linear Collider: the ZZ-fusion channel in the Standard Model

Stefano Moretti[1]

Dipartimento di Fisica Teorica, Università di Torino,
and I.N.F.N., Sezione di Torino,
Via Pietro Giuria 1, 10125 Torino, Italy.

Cavendish Laboratory, University of Cambridge,
Madingley Road, Cambridge, CB3 0HE, United Kingdom.

PACS numbers: 14.80.Bn, 14.70.Bh, 14.70.Hp, 29.17.+w.

Abstract

In this paper, we extend the analyses carried out in a previous article for WW-fusion to the case of Higgs production via ZZ-fusion within the Standard Model at the Next Linear Collider, in presence of electromagnetic radiation due real photon emission. Calculations are carried out at tree-level and rates of the leading order (LO) processes $e^+e^- \rightarrow e^+e^-H \rightarrow e^+e^-b\bar{b}$ and $e^+e^- \rightarrow e^+e^-H \rightarrow e^+e^-WW \rightarrow e^+e^-$jjjj are compared to those of the next-to-leading order (NLO) reactions $e^+e^- \rightarrow e^+e^-H(\gamma) \rightarrow e^+e^-b\bar{b}\gamma$ and $e^+e^- \rightarrow e^+e^-H(\gamma) \rightarrow e^+e^-WW(\gamma) \rightarrow e^+e^-$jjjj$\gamma$, in the case of energetic and isolated photons.

[1]E-mails: Moretti@to.infn.it; Moretti@hep.phy.cam.ac.uk.

In a previous paper [1] we studied the effects of hard photon emission in the WW-fusion reactions

$$e^+e^- \to \bar{\nu}_e\nu_e H(\gamma) \to \bar{\nu}_e\nu_e b\bar{b}\gamma, \tag{1}$$

$$e^+e^- \to \bar{\nu}_e\nu_e H(\gamma) \to \bar{\nu}_e\nu_e WW(\gamma) \to \bar{\nu}_e\nu_e \mathrm{jjjj}\gamma. \tag{2}$$

The production mechanism $e^+e^- \to \bar{\nu}_e\nu_e H$ and the decay channels $H \to b\bar{b}$, jjjj represent some of the most likely signatures of Higgs processes at the Next Linear Collider (NLC) [2]–[5], within the Standard Model ($\mathcal{SM}$), for a H scalar in the intermediate (1) and heavy (2) mass range (IMR and HMR, respectively)[2].

In that study we focused our attention to the case of hard and isolated photons. The motivation of that analysis came from the observation that the rôle of energetic photons from the initial state is expected to be determinant at the e^+e^- colliders of the next generation. In particular, whereas at LEP1, SLC and partially LEP2, the finite width of the gauge boson resonances heavily suppresses events with hard photons produced in the e^+e^- annihilation subprocess, at a high energy NLC (when $\sqrt{s} \gtrsim 300$ GeV) this is no longer true. Furthermore, since the energy of the beams is much larger, the probability that the incoming electrons and positrons radiate is somewhat bigger. Therefore, one naturally expects the NLC to produce rather copiously events accompanied by hard electromagnetic (EM) emission and these cannot be ignored in realistic phenomenological analyses.

In many instances, one can give account of the Initial State Radiation (i.e., bremsstrahlung of photons from the incoming electron/positron lines) by means of the so-called 'electron structure functions' [8]. In addition, for certain designs of the NLC, the effects due to such a radiation are dominant with respect to those due to beamsstrahlung and Linac energy spread phenomena [9]: such that, in phenomenological studies, one can consistently deal with bremsstrahlung photons only. However, on the one hand, this approach is realistically applicable only in the case of *annihilation*- and *conversion*-type Feynman diagrams: that is, when the $e^\pm$-lines are connected to each other via s- or t,u-channel interactions [10]. When the electron and positron lines are disconnected by gauge boson currents, like in the case of WW-fusion processes, a separation of the radiation emitted by the incoming fermion lines from that radiated by the virtual W-boson lines (see Fig. 1–2 in Ref. [1]) is indeed not gauge invariant. On the other hand, in experimental data, radiative events with photons coming from the Higgs production mechanism are not distinguishable from those in which they come from the Higgs decays.

To give reliable predictions for the corrections at the order $\mathcal{O}(\alpha_{\mathrm{em}})$ to the leading processes

$$e^+e^- \to \bar{\nu}_e\nu_e H \to \bar{\nu}_e\nu_e b\bar{b}, \tag{3}$$

[2]For a NLC with $\sqrt{s} \lesssim 500$ GeV and $M_H \lesssim 2M_W$ the production rates of the bremsstrahlung process $e^+e^- \to ZH$ are comparable or larger than those of the WW-fusion channel [6, 7].

$$e^+e^- \to \bar{\nu}_e\nu_e H \to \bar{\nu}_e\nu_e WW \to \bar{\nu}_e\nu_e \mathrm{jjjj}, \tag{4}$$

one should compute the contributions due to real photons as well as those due to virtual photons in the loop diagrams. Their summation through the orders $\mathcal{O}(\alpha_{\rm em}^5)$ and $\mathcal{O}(\alpha_{\rm em}^7)$ would allow one to cancel the infrared (soft and collinear) divergences appearing in the matrix elements (MEs). However, to compare the tree-level rates of the LO processes (3)–(4) with those of the NLO ones (1)–(2) for hard photons only, allows one to assess whether (at higher order) complications should be expected in working out the position of the resonances and/or in establishing their line-shape, or whether the overall effect of the complete $\mathcal{O}(\alpha_{\rm em})$ corrections will be in the end only matter of a different normalisation (of the LO spectra).

In the approach of Ref. [1], virtual photon contributions were ignored, for both the cases of what we called 'production radiation' and 'decay radiation'. (In detail, the first is due to photons emitted during the Higgs production mechanism, whereas the second refers to photons radiated in the Higgs decays, and they are separately gauge-invariant.) As loop diagrams were missing, the mentioned summation was not performed there. In that paper, we compared the rates of the lowest order processes (3) and (4) to those at next-to-lowest order from reactions (1) and (2) over the phase space regions defined by the cuts: $p_T^{b,\,\mathrm{j},\gamma} > 1$ GeV and $\cos\theta_{b\gamma,\,\mathrm{j}\gamma} < 0.95$. The aim was to make the point that in many instances (that is for various combinations of NLC centre-of-mass (CM) energies, $\sqrt{s}$, and Higgs masses, M_H) the rates of the hard radiative processes can be rather large compared to those of the leading reactions and that in some cases a complete $\mathcal{O}(\alpha_{\rm em})$ calculation would be desirable in order to assess the relative importance of events of the type (6) with hard photons, with respect to those in which the electromagnetic emission is either infrared or virtual and to the lowest order rates as well, as a shift in the position of the Higgs peaks could be expected at NLO (see again Ref. [1] for a fuller discussion). Another feature of interest to phenomenological analyses stressed in Ref. [1] is the fact that rather clear Higgs signals can appear in the spectra of the invariant masses $M_{b\bar{b}\gamma}$ and $M_{\mathrm{jjjj}\gamma}$. The last point outlined in Ref. [1] is that it is generally impossible to separate in radiative events (1)–(2) the 'production radiation' from the 'decay radiation', at least by exploiting the spectra in photon energy, E_γ, and in missing transverse momentum of the neutrino pair, $p_T^{\rm miss}$.

We intend in this brief report to perform studies similar to those of Ref. [1] for the case of a $\mathcal{SM}$ Higgs boson produced via the ZZ-fusion mechanism and decaying through the two mentioned channels, by studying the reactions:

$$e^+e^- \to e^+e^- H(\gamma) \to e^+e^- b\bar{b}\gamma, \tag{5}$$

$$e^+e^- \to e^+e^- H(\gamma) \to e^+e^- WW(\gamma) \to e^+e^- \mathrm{jjjj}\gamma, \tag{6}$$

$$e^+e^- \to e^+e^- H \to e^+e^- b\bar{b}, \tag{7}$$

$$e^+e^- \to e^+e^- H \to e^+e^- WW \to e^+e^- \mathrm{jjjj}. \tag{8}$$

As in this case infrared divergences can occur also in the bremsstrahlung of soft and collinear photons off the $e^{\pm}$-lines in the final state, we impose that $\cos\theta_{e/b\gamma,e/\ \mathrm{j}\gamma} < 0.95$ (that is, separation of the photon also from the outgoing electron/positron). Moreover, since the $e^{\pm}$-particles in the final states are detectable (contrary to the neutrinos in the WW-fusion), we ask $p_T^{e,b,\ \mathrm{j},\gamma} > 1$ GeV. The Feynman diagrams describing the reactions (5)–(6) at tree-level are the same pictured in Fig. 1–2 of Ref. [1], with graphs 5–6 there replaced by those in Figs. 1a–b of the present paper. Their calculation has been carried out in the same way as in Ref. [1], so we refer to that publication for all details.

We have verified that also in the case of the ZZ-fusion processes the spectra in photon energy and in missing transverse momentum of the e^+e^- pair show a similar behaviour to that described in case of processes (1)–(4). Therefore, we concentrate here only on the case of the integrated rates and in the invariant mass spectra $M_{b\bar{b}}$, M_{jjjj}, $M_{b\bar{b}\gamma}$ and $M_{\mathrm{jjjj}\gamma}$. Our results are presented in Figs. 2a–b and Figs. 3a–b. For consistency, the choice of the collider CM energies and Higgs masses we have adopted here is the same as in Ref. [1].

Many of the features typical of processes (1)–(4) are reproduced in case of processes (5)–(8) as well: yet, differential and integrated rates are here smaller by an order of magnitude at least (compare Figs. 2a–b to Figs. 3–4 of Ref. [1]), both at LO (as well known) and at NLO. Concerning the total cross sections, one can notice (Fig. 2a) that in the IMR the NLO contribution due to hard photons is never greater than $\approx 10\%$ of the LO rates, for all $\sqrt{s} = 300, 500$ and 1000 GeV, when M_H varies in the IMR. The same can be affirmed for a scalar with mass in the whole of the HMR (Fig. 2b).

Figs. 3a–b show the distribution in the invariant masses of the Higgs decay products: i.e., $M_{b\bar{b}(\gamma)}$ and $M_{\mathrm{jjjj}(\gamma)}$. Things are here very similar to the case of the corresponding WW-fusion processes, such that the same comments contained in Ref. [1] hold here too. However, a different feature of ZZ-fusion processes compared to the WW-fusion ones is that the relative contribution of graphs 5 and 6 to the total cross section at NLO is smaller in the former. This is due to the additional cut between the final state electron/positron and photon directions implemented in case of processes (5)–(6), as the EM emission along the $e^{\pm}$ lines tends to be highly collinear. This ultimately reduces the relevance of NLO hard photon events, compared to the lowest order rates. In fact, for the $b\bar{b}$ invariant masses (left plots in Fig. 3a), the smearing towards low values (that is, $M_{b\bar{b}} < M_H$) of the Higgs resonances due to the hard EM radiation in the $H \to b\bar{b}\gamma$ three-body decays induces an effect of only $\approx 1\%$ at the most, for all Higgs masses and collider energies. The suppression of the 'decay radiation' is once again visible also in the invariant mass of the $b\bar{b}\gamma$ system (plots on the right in Fig. 3a), because of the absence of clear Breit-Wigner peaks [1]. For a Higgs scalar in the HMR, we notice that the shape of the mass distributions on the left hand side of Fig. 3b is rather different at the two orders. The effect is visible at all energies: for example, see the open and shaded dotted histograms (see also Ref. [1]). However, the quantitative effect is rather small compared to the case of WW-fusion. Finally, Higgs peaks clearly appear in the $M_{\mathrm{jjjj}\gamma}$ spectra (right hand side of Fig. 3b).

Therefore, we conclude by remarking that the corrections due to hard photons in reactions induced by ZZ-fusion are generally smaller compared to the case of WW-fusion processes, both in the intermediate and heavy mass range of M_H. In particular then, when folding the real radiation computed here with the virtual one and with the lowest order rates to produce the complete result at the $\mathcal{O}(\alpha_{\mathrm{em}})$ higher order, the smearing of the resonant Higgs peaks should be less relevant than in the WW-fusion case, and negligible in general. However, in the HMR and especially for very large NLC energies (i.e., around and above 1000 GeV, see Fig. 3b bottom left), a complete NLO calculation would be desirable for phenomenological analyses that consider ZZ-fusion on its own. We finally notice that for ZZ-fusion Higgs processes (like for WW-fusion) the inclusion of four-jet decays via the ZZ-channel (i.e., $H \to ZZ \to \mathrm{jjjj}(\gamma)$) should reduce the relevance of hard radiative contributions; and that a careful treatment of the Higgs-strahlung process $e^+e^- \to ZH$ (followed by $Z \to e^+e^-$) and of its interference with the ZZ-fusion mechanism would be needed (see the discussions in the last two paragraphs of Section 3 in Ref. [1]). The last aspect is especially important when dealing with processes (5)–(8), as the LO rates of the two Higgs mechanisms (i.e., ZH-production and ZZ-fusion) are comparable for all combinations of $\sqrt{s}$ and M_H considered here (whereas WW-fusion always dominates for $\sqrt{s} \gtrsim 500$ GeV).

We are grateful to the UK PPARC for support. This work was financed in part by the Ministero dell' Università e della Ricerca Scientifica and by the EC Programme "Human Capital and Mobility", contract CHRX–CT–93–0357 (DG 12 COMA).

References

[1] S. Moretti, *preprint* DFTT 26/96, Cavendish–HEP–96/07, July 1996 (to be published in *J. Phys.* **G**).

[2] Proceedings of the Workshop "*Physics and Experiments with Linear Colliders*", Saariselkä, Finland, 9-14 September 1991, eds. R. Orawa, P. Eerola and M. Nordberg, World Scientific Publishing, Singapore, 1992.

[3] Proc. of the Workshop "*e^+e^- Collisions at 500 GeV. The Physics Potential* ", Munich, Annecy, Hamburg, 3-4 February 1991, ed. P.M. Zerwas, DESY pub. 92-123A/B, August 1992; DESY pub. 93-123C, December 1993.

[4] Proc. of the ECFA workshop on "*e^+e^- Linear Colliders LC92*", R. Settles ed., Garmisch Partenkirchen, 25 July-2 Aug. 1992, MPI-PhE/93-14, ECFA 93-154.

[5] Proc. of the I-IV Workshops on Japan Linear Collider (JLC), KEK 1989, 1990, 1992, 1994, KEK-Reports 90-2, 91-10, 92-1, 94-1.

[6] J.D. Bjorken, Proceedings of the "*Summer Institute on Particle Physics*", *SLAC Report* 198 (1976);
B.W. Lee, C. Quigg and H.B. Thacker, *Phys. Rev.* **D16** (1977) 1519;
J. Ellis, M.K. Gaillard and D.V. Nanopoulos, *Nucl. Phys.* **B106** (1976) 292;
B.L. Ioffe and V.A. Khoze, *Sov. J. Part. Nucl.* **9** (1978) 50.

[7] D.R.T. Jones and S.T. Petkov, *Phys. Lett.* **B84** (1979) 440;
R.N. Cahn and S. Dawson, *Phys. Lett.* **B136** (1984) 196;
K. Hikasa, *Phys. Lett.* **B164** (1985) 341;
G. Altarelli, B. Mele and F. Pitolli, *Nucl. Phys.* **B287** (1987) 205;
B. Kniehl, *preprint* DESY 91-128, 1991.

[8] F.A. Berends, W.L. van Neerven and G.J. Burgers, *Nucl. Phys.* **B297** (1988) 429; Erratum, *ibidem* **B304** (1988) 95;
E.A. Kuraev and V.S. Fadin, *Sov. J. Nucl. Phys.* **41** (1985) 466;
G. Altarelli and G. Martinelli, Proceedings of the Workshop '*Physics at LEP*', eds. J. Ellis and R. Peccei, Geneva, 1986, CERN 86-02;
R. Kleiss, *Nucl. Phys.* **B347** (1990) 29;
O. Nicrosini and L. Trentadue, *Phys. Lett.* **B196** (1987) 551; *Z. Phys.* **C39** (1988) 479.

[9] T. Barklow, P. Chen and W. Kozanecki, in Ref. [3], part B, and references therein.

[10] D. Bardin, D. Lehner and T. Riemann, *preprint* DESY 96-028, February 1996.

Figure Captions

Fig. 1 New Feynman diagrams at tree-level which substitute those corresponding to the WW-fusion channel when the photon is emitted by W bosons in the Higgs production mechanism (see diagrams 5–6 in Figs. 1–2 of Ref. [1]): (**a**) in case of process (5); (**b**) in case of process (6).

Fig. 2 Cross sections of the processes: (**a**) (5) and (7); (**b**) (6) and (8); as a function of the Higgs mass, at $\sqrt{s}$ = 300 GeV (upper plot), $\sqrt{s}$ = 500 GeV (central plot), $\sqrt{s}$ = 1000 GeV (lower plot), after the cuts $p_T^{e,h,\gamma} > 1$ GeV and $\cos\theta_{e/h\gamma} < 0.95$, where $h = b$ or j, as appropriate.

Fig. 3 Distributions in: (**a**) invariant mass of the $b\bar{b}$ (left plots) and of the $b\bar{b}\gamma$ (right plots) systems for processes (5) and (7), for $M_H = 60, 100, 140$ GeV at $\sqrt{s} = 300(500)[1000]$ GeV; (**b**) invariant mass of the jjjj (left plots) and of the jjjjγ (right plots) systems for processes (6) and (8), for $M_H = 180, 220, 260(180, 260, 340)[180, 300, 420]$ GeV at $\sqrt{s} = 300(500)[1000]$ GeV. The following cuts have been applied: $p_T^{e,h,\gamma} > 1$ GeV and $\cos\theta_{e/h\gamma} < 0.95$, where $h = b$ or j, as appropriate. The values of the CM energy are: $\sqrt{s} = 300$ GeV (upper plots, bins of 2 GeV); $\sqrt{s} = 500$ GeV (central plots, bins of 4 GeV); $\sqrt{s} = 1000$ GeV (lower plots, bins of 5 GeV). In the left plots the upper histograms refer to rates from the non-radiative processes (7) and (8), whereas the lower histograms correspond to rates from the radiative processes (5) and (6). The latter are shaded.

Diagrams by MadGraph

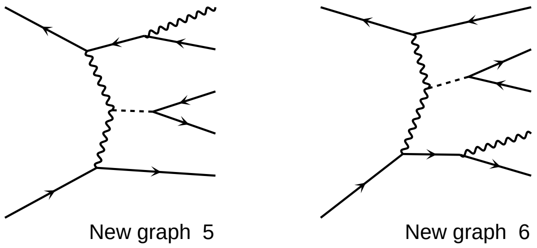

Fig. 1a

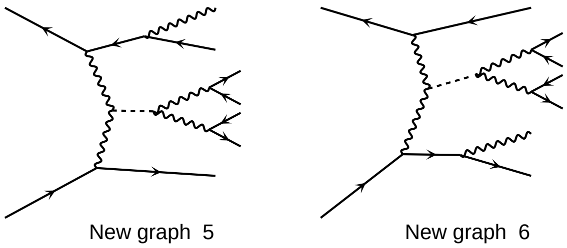

Fig. 1b

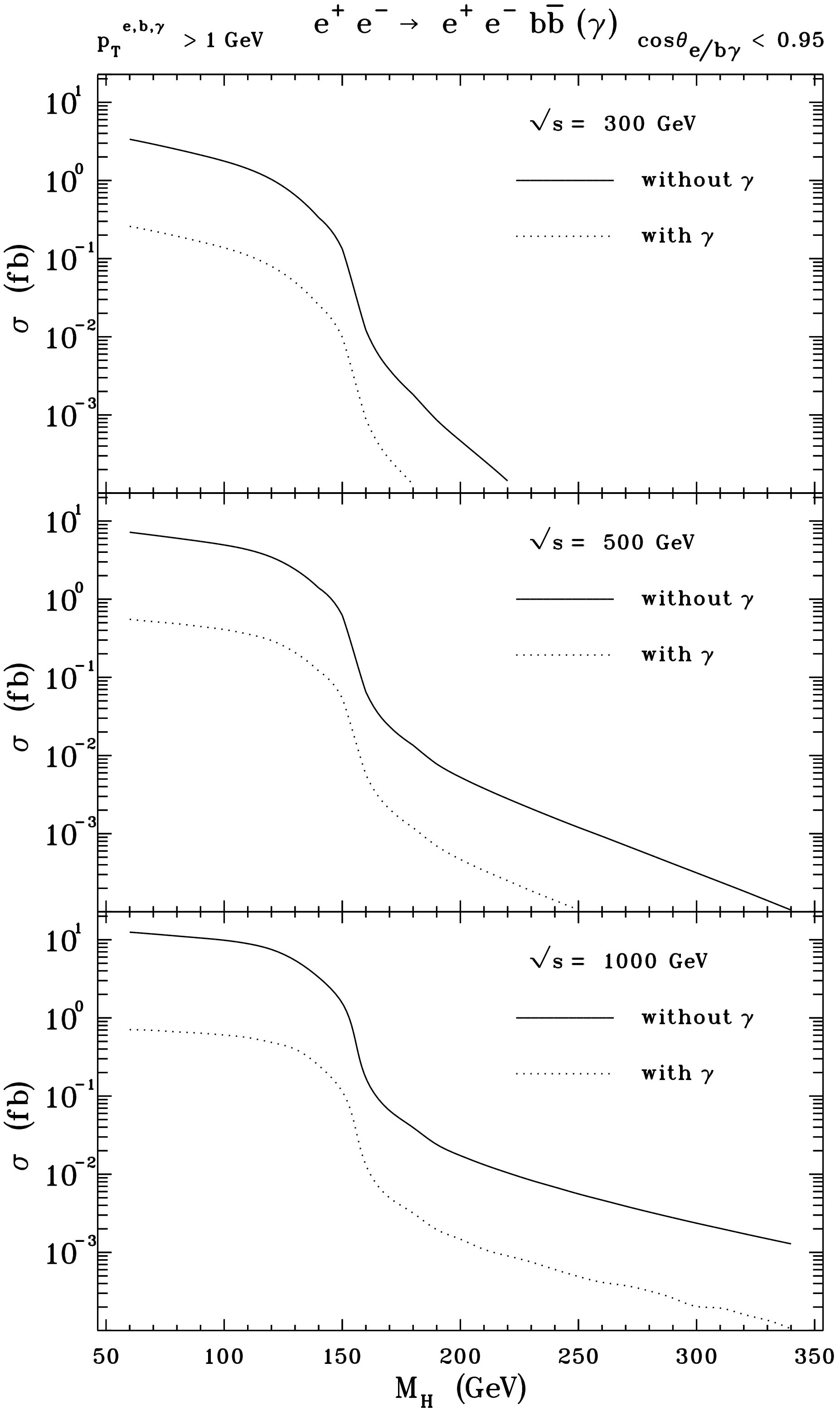
$p_T^{e,b,\gamma} > 1$ GeV
$e^+ e^- \to e^+ e^- b\bar{b}\ (\gamma)$
$\cos\theta_{e/b\gamma} < 0.95$
$\sqrt{s} =$ 300 GeV
without γ
with γ
$\sqrt{s} =$ 500 GeV
without γ
with γ
$\sqrt{s} =$ 1000 GeV
without γ
with γ
σ (fb)
10^1
10^0
10^{-1}
10^{-2}
10^{-3}
50
100
150
200
250
300
350
M_H (GeV)

Fig. 2a

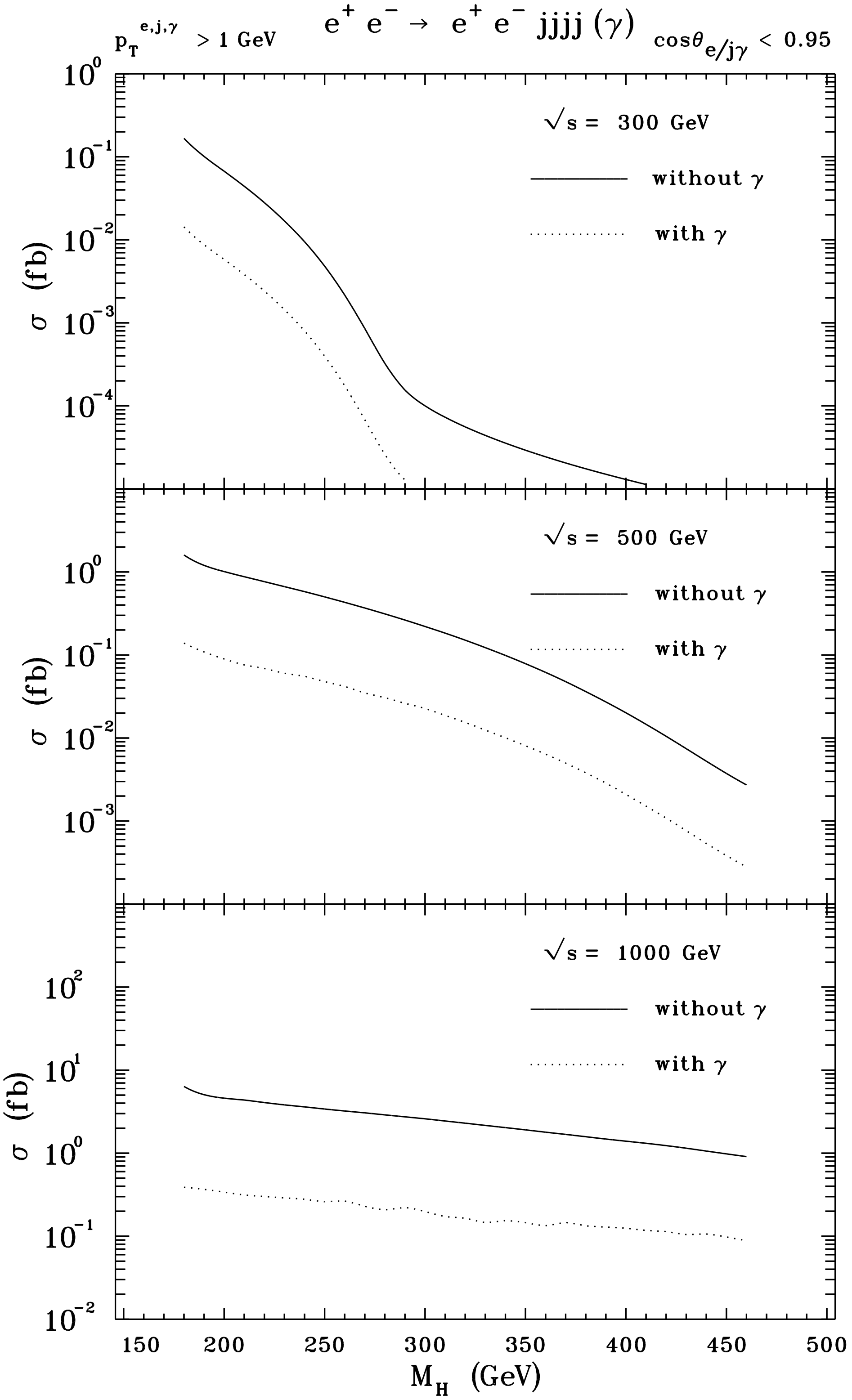
$p_T^{e,j,\gamma} > 1$ GeV
$e^+ e^- \to e^+ e^- jjjj\,(\gamma)$
$\cos\theta_{e/j\gamma} < 0.95$
$\sqrt{s} =$ 300 GeV
$\sqrt{s} =$ 500 GeV
$\sqrt{s} =$ 1000 GeV
without γ
with γ
σ (fb)
M_H (GeV)
150
200
250
300
350
400
450
500

Fig. 2b

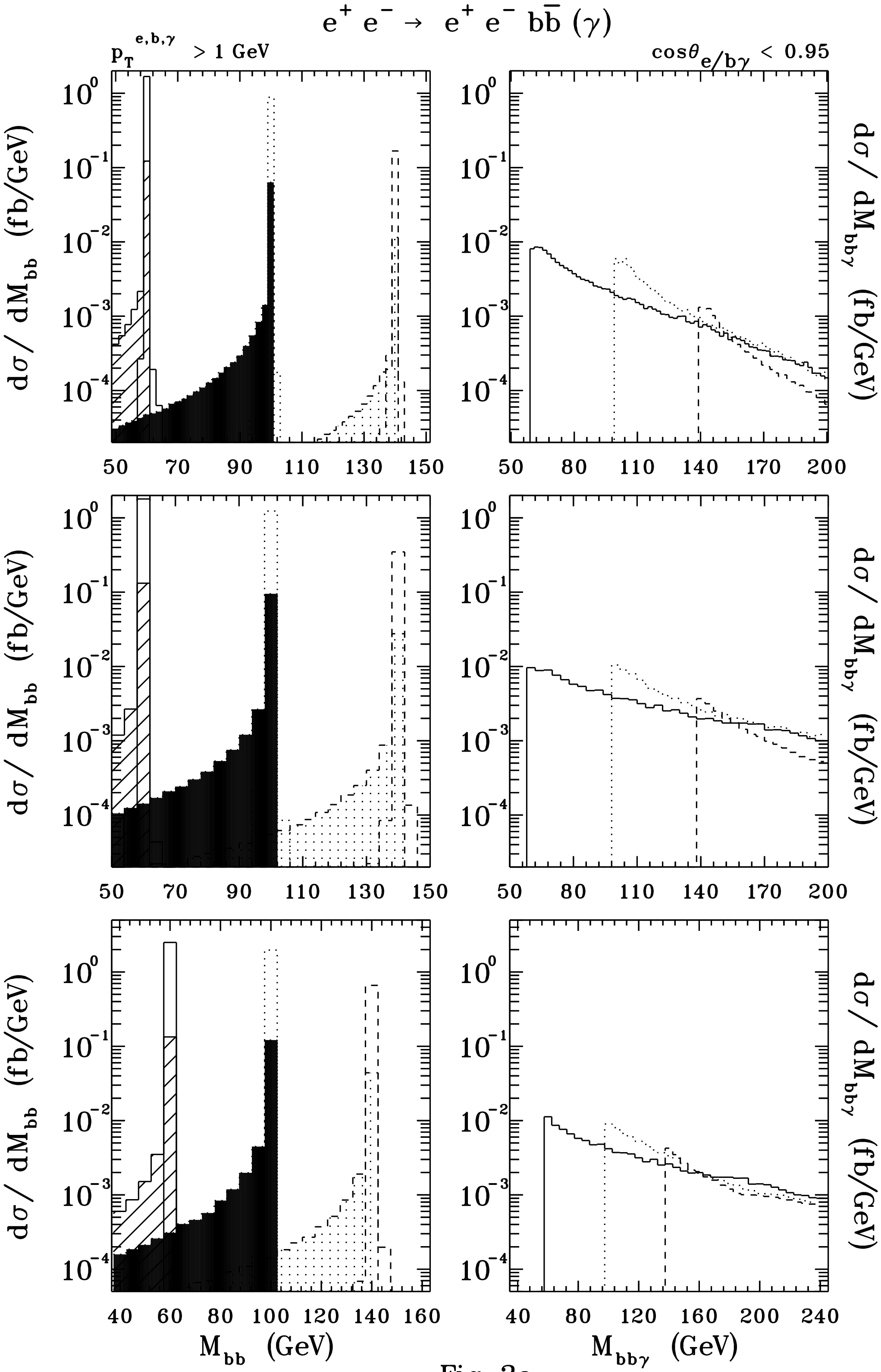

$e^+ e^- \rightarrow e^+ e^- b\bar{b}\,(\gamma)$
$p_T^{e,b,\gamma} > 1$ GeV
$\cos\theta_{e/b\gamma} < 0.95$
$d\sigma/dM_{bb}$ (fb/GeV)
$d\sigma/dM_{bb\gamma}$ (fb/GeV)
M_{bb} (GeV)
$M_{bb\gamma}$ (GeV)

Fig. 3a

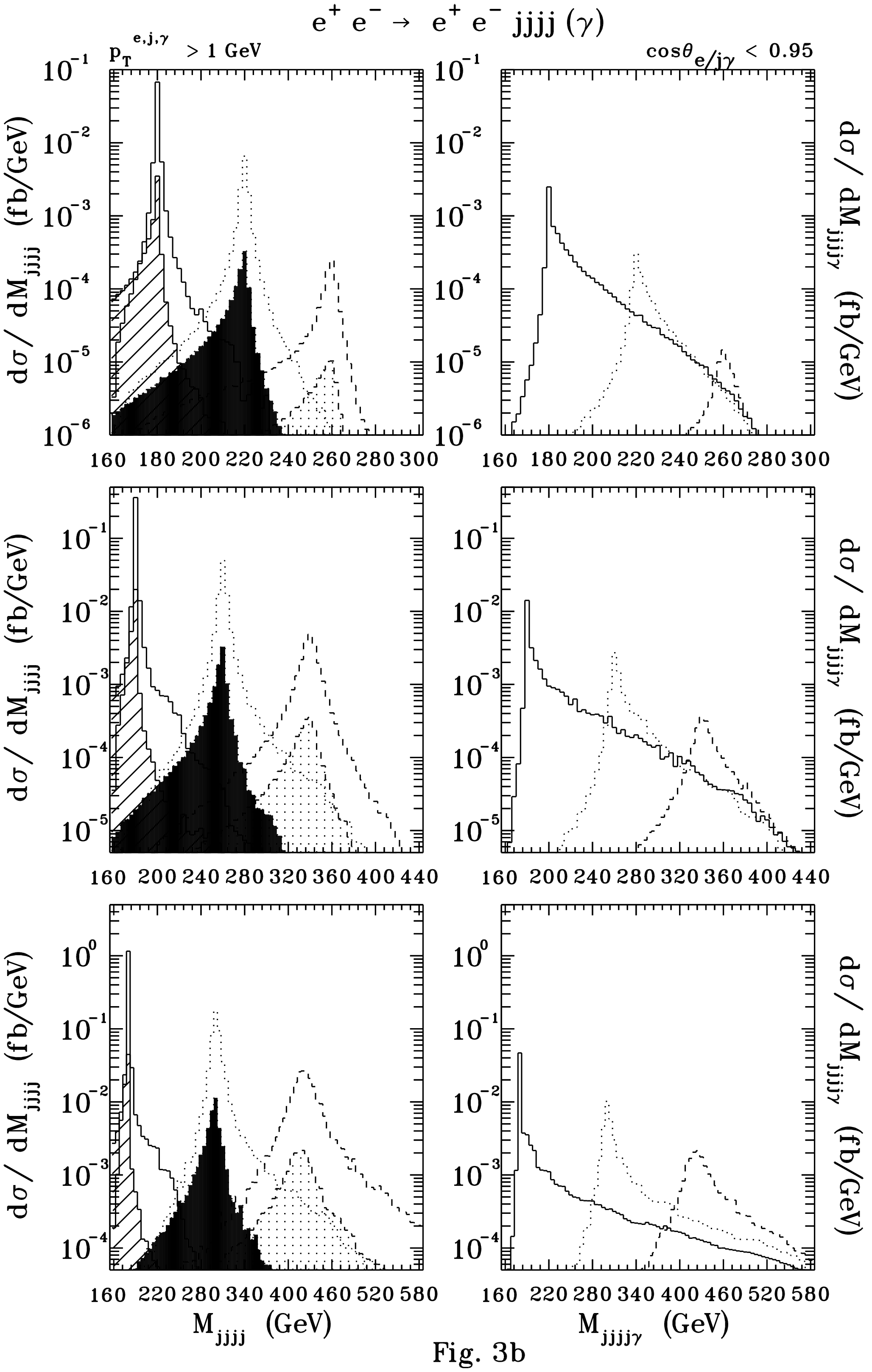

$e^+ e^- \to e^+ e^- jjjj\,(\gamma)$
$p_T^{e,j,\gamma} > 1$ GeV
$\cos\theta_{e/j\gamma} < 0.95$
$d\sigma / dM_{jjjj}$ (fb/GeV)
$d\sigma / dM_{jjjj\gamma}$ (fb/GeV)
M_{jjjj} (GeV)
$M_{jjjj\gamma}$ (GeV)

Fig. 3b